Thermal Rearrangements of Di- and Triphenyl-Substituted Benzocyclobutenes and Corresponding *o*-Quinodimethanes

Thomas Paul,[a] Roland Boese,[b] Ingo Steller,[b] Heinz Bandmann,[a] Georg Gescheidt,[c] Hans-Gert Korth,*[a] and Reiner Sustmann*[a]

In memoriam Wolfgang R. Roth

Keywords: Benzocyclobutenes / *o*-Quinodimethanes / Pericyclic reactions / Retrodisproportionation / 9-Anthryl radicals

7,8-Dimethoxy-7,8-diphenyl- (**1c**), 7,8-dimethyl-7,8-diphenyl- (**1d**), 7-methoxy-7,8,8-triphenyl- (**1e**), 7-methyl-7,8,8-triphenyl- (**1f**), 7-isocyano-7,8,8-triphenyl- (**1g**), and 7,7,8-triphenylbenzocyclobutene (**1h**) are amenable to a variety of thermal rearrangements following initial electrocyclic ring-opening to the corresponding 7,8-diphenyl- (**2c**,**d**) and 7,8,8-triphenyl-*o*-quinodimethanes (**2e–h**). *meso*-**1c** was found to undergo a facile *meso*/*rac* isomerization at room temperature, indicating that other processes such as a symmetry-forbidden disrotatory ring-opening or a stepwise reaction compete with the symmetry-allowed conrotatory process. An estimate of the energy profile of the **1c**/**2c** reaction system was made by kinetic simulation in combination with oxygen trapping of the intermediate *o*-quinodimethanes (**2c**) and semiempirical PM3 calculations, and revealed that the barrier for the symmetry-forbidden pathway is merely about 4 kJ·mol^{-1} higher than that for the symmetry-allowed one. *o*-Quinodimethanes **2c**, **2g**, **2e**, and **2h** underwent further electrocyclic hexatriene-cyclohexadiene ring-closure to give 4a,10-dihydroanthracene derivatives at temperatures between 20 and 80 °C. The 4a,10-dihydroanthracenes were further transformed to 9,10-disubstituted anthracenes by elimination of methanol or HCN, as well as to 9,10-substituted 9,10-dihydroanthracene derivatives. ESR and ENDOR spectroscopic detection of related 9-anthryl radicals lends support to the view that 9,10-dihydroanthracene products are formed by a homolytic hydrogen-transfer reaction (retrodisproportionation). By way of contrast, the aforementioned transformations play only a minor role in the case of methyl-substituted benzocyclobutenes **1d**, **1f** as here they are overruled by faster 1,5-H shift reactions of the corresponding *o*-quinodimethanes **2d**, **2f**, leading to styrene derivatives.

Introduction

The mutual, thermal interconversion of benzocyclobutenes (**1**) and *o*-quinodimethanes (**2**),[1] one of the classical examples of a concerted, electrocyclic process in the framework of the rules of conservation of orbital symmetry,[2] is generally believed to proceed in a conrotatory fashion.[3] For symmetrically 7,8-disubstituted benzocyclobutenes, such as 7,8-diphenylbenzocyclobutene (**1a**, R = Ph), a conrotatory electrocyclic process would result in the preservation of the *meso* or *rac* stereochemistry of the starting material (Scheme 1).[4]

Any *meso*/*rac* isomerization of such benzocyclobutenes would, therefore, require either a disrotatory ring-opening or -closure (if the isomerization were to proceed in a concerted mode) or rotation about only one of the active bonds in the benzocyclobutenes **1** or *o*-quinodimethanes **2**.

It is interesting to note that non-stereospecific *meso*/*rac* isomerization of 7,8-disubstituted benzocyclobutenes was briefly mentioned in some early papers,[3,4] but to the best of our knowledge it is only recently that this process has been investigated in detail for two prototypal systems, namely 7,8-diphenyl- (**1a**, R = Ph) and 7,8-dimethylbenzocyclobutene (**1b**, R = Me).[5]

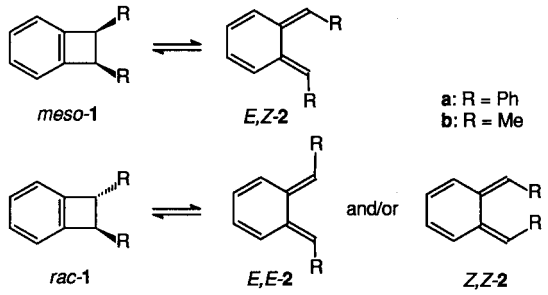

Scheme 1. Conrotatory ring-opening of benzocyclobutenes

In a recent paper[6] we reported on the photolytic decomposition of 1,3-diphenyl- and 1,1,3-triphenyl-substituted 2-indanones **3** and on the reaction of their photoproducts, benzocyclobutenes **1** and *o*-quinodimethanes **2**, with nitric oxide in order to assess their potential to serve as *nitric oxide cheletropic traps* (NOCTs)[7] allowing ESR detection of the resulting nitroxides **4** (Scheme 2).

In the course of these studies we observed that some of our benzocyclobutenes underwent facile ring-opening to *o*-quinodimethanes **2**, even at ambient temperature (Scheme 3). Subsequently, further rearrangements and hydrogen-

[a] Institut für Organische Chemie, Universität Essen, Universitätsstrasse 5, D-45117 Essen, Germany
Fax: (internat.) +49 (0)201/183-3096
E-mail: sustmann@oc1.orgchem.uni-essen.de
[b] Institut für Anorganische Chemie, Universität Essen, Universitätsstrasse 5, D-45117 Essen, Germany
[c] Institut für Physikalische Chemie, Universität Basel, Klingelbergstrasse 80, CH-4056 Basel, Switzerland

  1434–193X/99/0303–0551 $ 17.50+.50/0

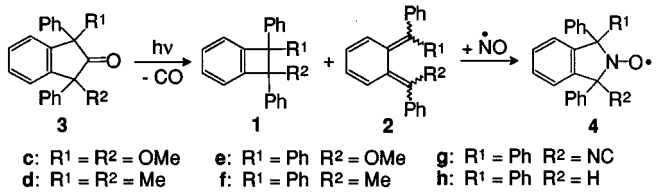

Scheme 2. NO trapping of *o*-quinodimethanes

transfer reactions took place. These included symmetry-forbidden thermal *meso*/*rac* isomerization (in the case of the symmetrically substituted 7,8-diphenylbenzocyclobutene **1c**), 1,5-hydrogen shift to produce styrene derivatives **5** (from **1d** and **1f**), and electrocyclic ring-closure to give 4a,10-dihydroanthracenes **6** (from **1c** and **1e**−**h**). Compounds **6** were further transformed to 9,10-substituted anthracene (**7**) and 9,10-substituted 9,10-dihydroanthracene (**8**) derivatives, in the course of which process substituted 9-anthryl radicals (**9**) could be detected by ESR. Although some of these reaction pathways have been known for quite some time,[1,3,8] detailed kinetic and mechanistic analyses are scarce.[5] Here, we present a spectroscopic and kinetic investigation of some of these reactions.

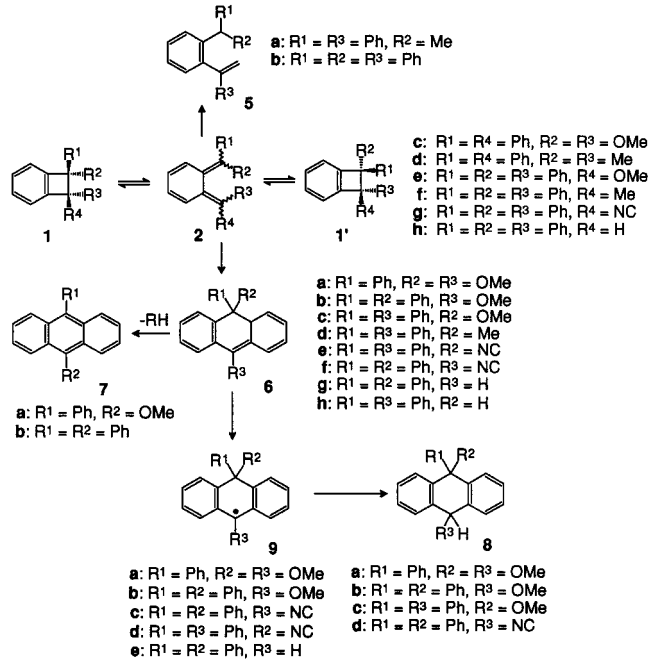

Scheme 3. Thermal rearrangements of phenyl-substituted benzocyclobutenes **1** via *o*-quinodimethanes **2**

Results

7,8-Dimethoxy-7,8-diphenylbenzocyclobutene (1c)

Owing to its favourable thermal stability, this compound was investigated most thoroughly. Compound **1c** was obtained as a 95:5 *meso*/*rac* mixture by photolytic decarbonylation of pure *meso*-**3c** in acetonitrile solution.[6] The fact that the configuration of the starting ketone is largely preserved during the photolysis indicates that decarbonylation and ring-closure occur very rapidly. From the photolysis mixture, pure *meso*-**1c** was isolated by fractional crystallization. The stereochemistry of the product was verified by X-ray structural analysis (Figure 1).

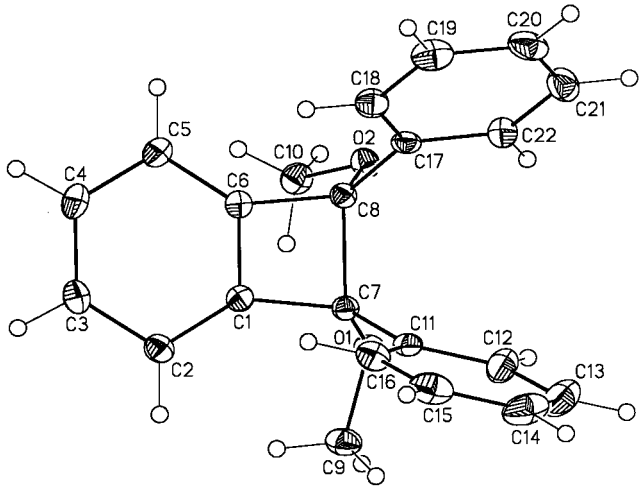

Figure 1. X-ray crystal structure of *meso*-**1c**

Whereas solid *meso*-**1c** is stable at room temperature, in solution it undergoes slow conversion to *rac*-**1c**, as can be monitored spectrometrically by ^{1}H- and ^{13}C-NMR in [D_3]acetonitrile solution. In oxygen-free solution, a *meso*−*rac* equilibrium was attained after about 2000 h at 20°C, with an equilibrium constant of K(*rac*-**1c**/*meso*-**1c**) = 7.5, corresponding to a $\Delta_R G°$ of −4.9 kJ·mol^{-1}.

As mentioned above, two borderline mechanistic schemes (Scheme 4, framed areas) can be envisaged to account for the *meso*/*rac* interconversion of **1c**: First, if ring-opening/ring-closure follows exclusively the conrotatory pathway, then the symmetry-forbidden process must result from a one-bond rotation (*E,Z*-**2c**/*Z,Z*-**2c** isomerization) in the intermediate *o*-quinodimethanes (Scheme 4a, framed area). Second, if the latter isomerization does not take place, then a symmetry-forbidden disrotatory ring-opening or ring-closure reaction in competition with the conrotatory process must be assumed (Scheme 4b, framed area). Schemes 4a and 4b cannot be distinguished kinetically by monitoring the time dependence of *meso*- and *rac*-**1c**. Thus, the experimental concentration-time data (Figure 2) could be fitted equally well to both simplified reaction schemes with the aid of a kinetic simulation procedure.[9] In both schemes, we neglect the fact that true biradical intermediates[5] might be involved in the isomerization process (see Discussion). For comparison purposes, the calculated rate constants for both schemes are collected in Table 1.

The significance of the magnitudes of the rate constants in Table 1 lies in the fact that the simulations predict, in agreement with the failure to detect **2c** by conventional ^{1}H-NMR spectrometry and our previous UV/vis spectroscopic and nitric oxide trapping experiments,[6] that the stationary concentration of the putative *o*-quinodimethane intermediates **2c** never exceeds 10^{-5} M over the entire time of 2000 h required for the *meso*/*rac* equilibration.

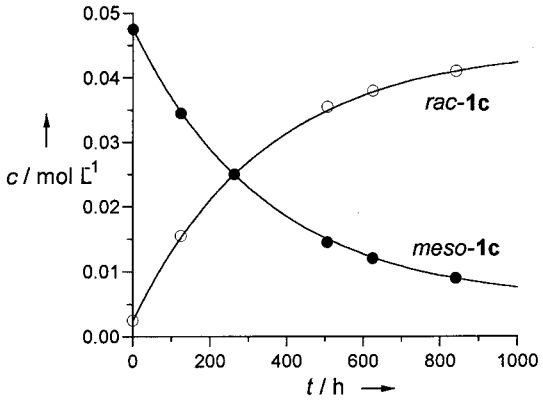

Figure 2. *meso*/*rac* Isomerization of **1c** (0.05 M) at 20°C in [D_3]acetonitrile; continuous curves: simulation according to the framed part of Scheme 4b

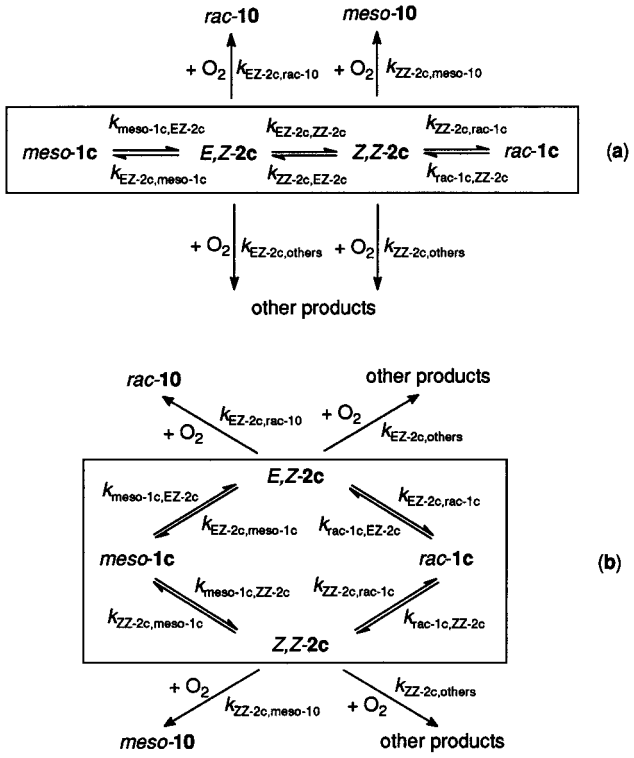

Scheme 4. Borderline kinetic schemes for the *meso*/*rac* isomerization of **1c** in the absence (framed areas) and presence of oxygen

Evidence for the formation of short-lived *o*-quinodimethanes can be obtained by the facile reaction of these species with nitric oxide[6,7] (Scheme 2) or, alternatively, by trapping with molecular oxygen, as has been demonstrated by Roth and co-workers.[5,10] Therefore, the isomerization of *meso*-**1c** was also carried out in the presence of molecular oxygen. In oxygen-saturated [D_3]acetonitrile solution, a variety of new ^{1}H- and ^{13}C-NMR resonances appeared over a period of days at 20°C. The principal (non-aromatic) signals were consistent with the predicted formation of the diastereomeric, cyclic peroxides *meso*- and *rac*-**10** (61 mol% combined yield) (Scheme 5), in a molar ratio varying from about 2.7 to 1.1 over the reaction period (100 d). The formation of two peroxides was confirmed by TLC of the reaction mixture, where two adjacent spots giving a positive peroxide test[11] were detected. Unfortunately, peroxides **10** turned out to be too unstable to be purified by preparative TLC or column chromatography. Decomposition seemingly occurred using either silica or alumina as the stationary phase, since significant amounts of *rac*-**1c** (up to 70%) were invariably recovered. The tentative assignment of the principal component of **10** as the *rac*-diastereomer is based on the reasonable assumption that the conrotatory ring-opening of *meso*-**1c** should be somewhat faster than a possible disrotatory one (see Discussion), and thus (*E*,*Z*)-**2c** should have been predominantly formed and trapped by O_2.[5]

Table 1. Rate constants at 20°C from the kinetic simulation of Schemes 4a, 4b

Rate constants	Scheme 4a[a]	Scheme 4b[a]	Scheme 4a[b]	Scheme 4b[b]
$k_{meso\text{-}1c,EZ\text{-}2c}$[c]	$1.4\cdot10^{-6}$	$1.4\cdot10^{-6}$	$1.8\cdot10^{-6}$	$1.4\cdot10^{-6}$
$k_{meso\text{-}1c,ZZ\text{-}2c}$[c]	–	$2.8\cdot10^{-7}$	–	$1.1\cdot10^{-6}$
$k_{EZ\text{-}2c,meso\text{-}1c}$[c]	$2.8\cdot10^{-3}$	$4.2\cdot10^{-3}$	$3.3\cdot10^{-3}$	$5.3\cdot10^{-3}$
$k_{ZZ\text{-}2c,meso\text{-}1c}$[c]	–	$3.9\cdot10^{-3}$	–	$3.9\cdot10^{-3}$
$k_{rac\text{-}1c,ZZ\text{-}2c}$[c]	$4.7\cdot10^{-7}$	$2.5\cdot10^{-7}$	$1.4\cdot10^{-6}$	$2.5\cdot10^{-7}$
$k_{rac\text{-}1c,EZ\text{-}2c}$[c]	–	$6.9\cdot10^{-8}$	–	$9.2\cdot10^{-8}$
$k_{ZZ\text{-}2c,rac\text{-}1c}$[c]	$1.1\cdot10^{-2}$	$1.1\cdot10^{-2}$	$1.9\cdot10^{-2}$	$8.1\cdot10^{-3}$
$k_{EZ\text{-}2c,rac\text{-}1c}$[c]	–	$2.8\cdot10^{-3}$	–	$2.8\cdot10^{-3}$
$k_{EZ\text{-}2c,ZZ\text{-}2c}$[c]	$8.3\cdot10^{-3}$	–	$8.3\cdot10^{-3}$	–
$k_{ZZ\text{-}2c,EZ\text{-}2c}$[c]	$5.6\cdot10^{-3}$	–	$5.6\cdot10^{-3}$	–
$k_{EZ\text{-}2c,rac\text{-}10}$[d]	–	–	$2.3\cdot10^{-1}$	$4.4\cdot10^{-1}$
$k_{ZZ\text{-}2c,meso\text{-}10}$[d]	–	–	$2.3\cdot10^{-1}$	$4.3\cdot10^{-1}$
$k_{EZ\text{-}2c,others}$[d]	–	–	$4.2\cdot10^{-2}$	$6.1\cdot10^{-2}$
$k_{ZZ\text{-}2c,others}$[d]	–	–	$3.3\cdot10^{-2}$	6.1·10

[a] In oxygen-free solution. – [b] At $8.1\cdot10^{-3}$ M O_2. – [c] [s^{-1}]. – [d] [M^{-1} s^{-1}].

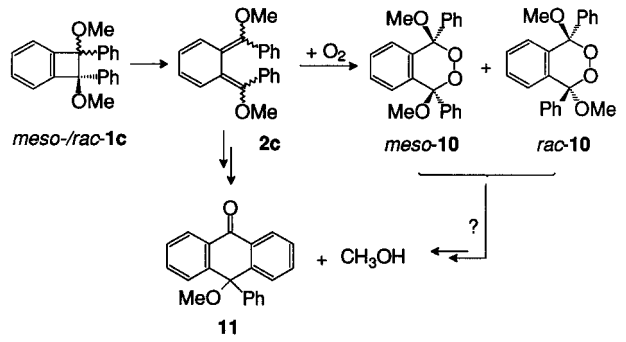

Scheme 5. Oxygen trapping of *o*-quinodimethanes **2c**

10-Methoxy-10-phenylanthrone (**11**)[12] and methanol were identified as by-products in yields of 16 and 14 mol%, respectively, after 100 d.

The time course of the *meso*-to-*rac* conversion of **1c** in the presence of oxygen was followed by monitoring the ^{1}H-NMR signals of the methoxy groups in the $\delta = 2.5-4$ region (Figure 3), with the sum of their integrals accounting for the mass balance (there was no indication that the methoxy groups themselves were subject to any chemical transformation).

The shape of the kinetic traces implied that **11** and methanol originated from unspecified reactions of the intermediates **2c** with oxygen rather than from further decomposition

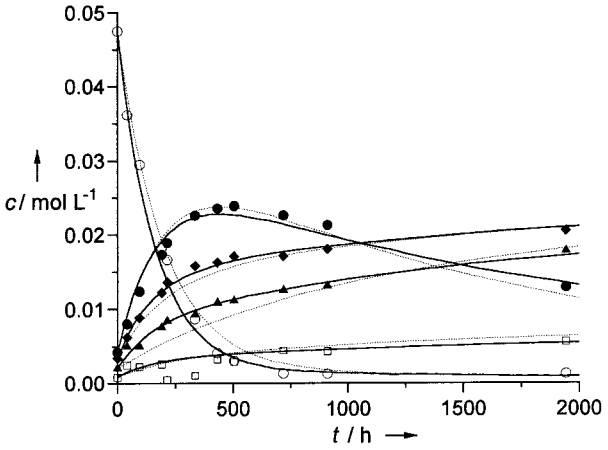

Figure 3. Decay of *meso*-**1c** (0.05 M) at 20°C in oxygen-saturated [D_3]acetonitrile solution; (○): *meso*-**1c**, (●): *rac*-**1c**, (◆): *meso*-**10**, (▲): *rac*-**10**, (□): other products. Lines: simulation according to Scheme 4a (dashed) and Scheme 4b (solid)

of the peroxides **10**. Though the latter decay path cannot be ruled out, the concentration-time profile shown in Figure 3 was analyzed in terms of the reactions depicted in Schemes 4a and 4b, respectively, by kinetic simulation.[9] Here, "other products" stands for the sum of anthrone **11**, methanol, and further minor, non-identified by-products. Again, the possibility of biradical intermediates was neglected. Furthermore, possible reversibility of the **2c** → **10** reactions, non-specific decay of peroxides **10** (to form "other" products), and/or possible *meso*/*rac* isomerization of **10** were not taken into account.

At a stationary O_2 concentration of $8.1 \cdot 10^{-3}$ M,[13] the fitting procedure yielded the rate constants shown in Table 1. A better fit with the experimental data was achieved using Scheme 4b as a basis (see Figure 3). Decay of *meso*-**1c** in air-equilibrated [D_3]acetonitrile solution gave a similar concentration-time profile. Here, in accordance with the lower steady-state level of oxygen ($1.9 \cdot 10^{-3}$ M[13,14]), formation of **10** was about four times slower, with the amount of *rac*-**1c** going through a maximum of about 60 mol% after 42 d (data not shown).

Whereas in the absence of oxygen at room temperature the *meso*/*rac* isomerization of **1c** proceeded without accumulation of any ^{1}H-NMR-detectable (≥ 0.1%) intermediates or by-products, heating of the samples to temperatures above 50°C resulted in the slow build-up of a variety of new ^{1}H-NMR resonances. Several weak, complex line patterns in the δ = 5.0−6.5 region pointed to the formation of diastereomeric 4a,10-dihydroanthracenes **6a** (Scheme 6) in an approximate 2.6:1 molar ratio. These signals disappeared upon prolonged (> 1 h) heating at 80°C. The intermediacy of **6a** was further supported by similar changes in the UV/vis absorptions in the 350−410 nm range, typical for 4a,10-dihydroanthracenes.[6,15] After 30 h at 80°C, **1c** and **6a** had almost completely decayed, leaving only several singlet lines in the non-aromatic region of the ^{1}H-NMR spectrum, the majority of which were identified as being due to the *syn*- and *anti*-diastereomers of the 9,10-dihydroanthracene derivative **8a** (75 and 8 mol%, respectively; the tentative assignment of the stereoisomers is based on PM3-calculated heats of formation, see Discussion). In addition, 9-methoxy-10-phenylanthracene (**7a**) (16 mol%) was identified from its known ^{1}H-NMR resonances.[12a,12b] In accordance with the proposed formation of **7a** by methanol elimination from **6a**, a comparable amount of methanol (12 mol%) was detected by "spiking" of the corresponding ^{1}H-NMR signal. The time-concentration profile is displayed in Figure 4.

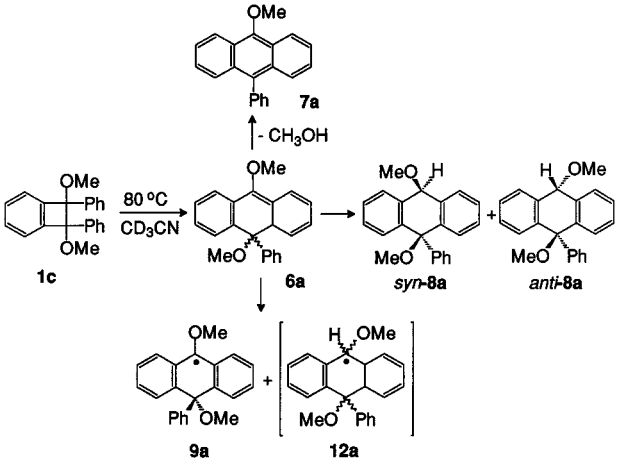

Scheme 6. Thermolysis of **1c** at 80°C

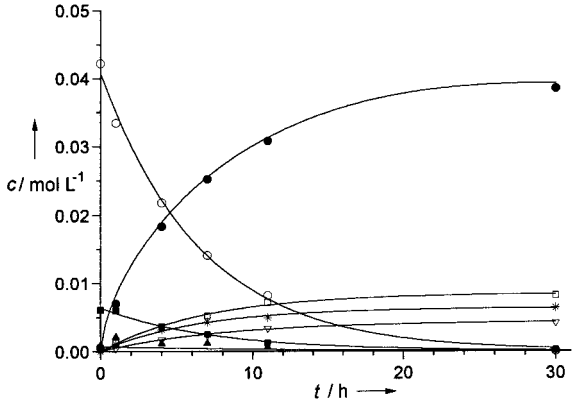

Figure 4. Thermolysis of the *meso*/*rac*-**1c** equilibrium mixture at 80°C in oxygen-free [D_3]acetonitrile; (○): *rac*-**1c**, (●): *syn*-**8a**, (■): *meso*-**1c**, (▲): **6a**, (□): **7a**, (▽): *anti*-**8a**, (*): methanol. Continuous lines: simulation according to Scheme 7.

As will be reported below, during decay of some of our benzocyclobutenes we observed ESR spectra of long-lived 9-anthryl radicals (**9**) (Scheme 3), which implied that the conversion of **6a** to **8a** might have been initiated by a bimolecular hydrogen-transfer reaction of **6a**, a process termed "retrodisproportionation" by Rüchardt and co-workers.[16] The likelihood of such a process in the present case was corroborated by the observation of a multi-line ESR spectrum when a sample of **1c** in diphenyl ether was heated to temperatures above 150°C. Though the low signal-to-noise ratio prohibited a detailed spectral analysis, the ESR spectrum was most probably due to the 9,10-dimethoxy-10-phenyl-9-anthryl radical (**9a**) (Scheme 6). Its overall width and the major hyperfine splittings (Table 3) resembled those

of the related spectra described below. Radical **12a** is an expected intermediate of the retrodisproportionation process (see Discussion, Scheme 9).

Kinetic simulation of the concentration-time profile in terms of the simplified reaction scheme (Scheme 7) provided the rate constants listed in Table 2. In agreement with the ^{1}H-NMR observations, the concentration of 4a,10-dihydroanthracene **6a** is predicted to pass through a minute maximum within 1 h.

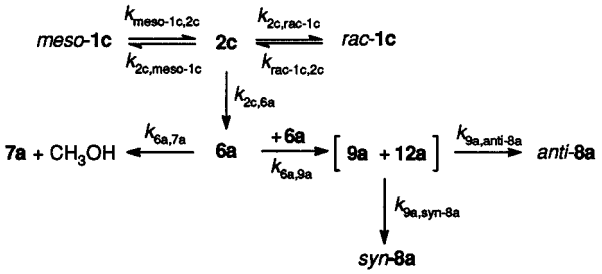

Scheme 7. Kinetic scheme for the thermolysis of **1c** at 80°C

7,8-Dimethyl-7,8-diphenylbenzocyclobutene (1d)

This compound was obtained as a 1:1.2 *meso*/*rac* mixture upon photolysis of **3d** in acetonitrile solution.[6] At ambient temperature, no change in the diastereomeric ratio was indicated by ^{1}H-NMR in [D_3]acetonitrile solution over a period of several days, nor were other products detected. On heating the solution to 60°C, **1d** underwent a smooth transformation to α-phenyl-*o*-(1-phenylethyl)styrene (**5a**) (Scheme 3), indicating that ring-opening to **2d** was followed by a rapid 1,5-H shift. After 27 h at 60°C, about 45% of the **1d** had been converted to **5a** [k(**1d**)^{353} = 8.2·10^{-6} s^{-1}], and the *meso*/*rac* ratio had changed to about 1:3. ^{1}H-NMR signals that might have been expected if an electrocyclic ring-closure to a corresponding 4a,10-dihydroanthracene derivative had occurred, could not be detected.

7-Methoxy-7,8,8-triphenylbenzocyclobutene (1e)

Due to the absence of a second chiral center in **1e**, the probable symmetry-forbidden electrocyclic ring-opening or -closure cannot be probed by *meso*/*rac* interconversion. However, rapid ring-opening of **1e** to *o*-quinodimethane **2e** in acetonitrile solution at 30°C was evident from the development of the ^{1}H-NMR signals of dihydroanthracenes **6b** and **6c** (two diastereomers), and those of methanol. Compound **1e** decayed with a rate constant of k(**1e**)^{303} = 3.1·10^{-5} s^{-1}, and the disappearance of the ^{1}H-NMR signals was paralleled by the development of a UV/vis absorption at λ_{max} = 384 nm, typical for dihydroanthracenes of type **6**.[1,15] These dihydroanthracenes appeared to be rather persistent; after 24 h (94% conversion of **1e**) the yields of **6b**, of the two diastereomers of **6c**, and of methanol amounted to 40, 19, 18, and 16 mol%, respectively. The "18%-isomer" of **6c** underwent further decay within 8 days, which was accompanied by an equivalent increase in the methanol content and the formation of 9,10-diphenylanthracene (**7b**) (identified by HPLC and UV/vis, λ_{max} = 338, 354, 373, and 393 nm,[17] by comparison with authentic material). NMR peaks that would have indicated the production of dihydroanthracenes **8b** and/or **8c** at levels of ≥ 1% could not be detected. By way of contrast, when the decay of **1e** was followed at the same temperature in [D_6]DMSO solution [k(**1e**)^{303} = 4.5·10^{-5} s^{-1}], only very weak ^{1}H-NMR signals of dihydroanthracenes **6** were detected, but in this case dihydroanthracenes **8b** and **8c** (two diastereomers, ratio ca. 8.5:1) were identified as the major products, in yields of 40 and 39 mol%, respectively, after 27 h (99% conversion of **1e**). The material balance was accounted for by several minor, unidentified by-products.

When the decomposition of **1e** in acetonitrile solution was performed in the cavity of the ESR spectrometer at 20°C, the slow evolution of a highly persistent, multi-line ESR spectrum was observed. The hyperfine splittings (hfs) were determined by ENDOR spectroscopy in diphenyl ether solution (Figure 5). The ENDOR data allowed the simulation of the ESR spectrum (Figure 6), where inclusion of one large ^{13}C-isotope splitting greatly improved the fit with the experimental spectrum. The ENDOR/ESR hfs data (Table 3) unambiguously identified the spectrum as being due to the 9-methoxy-10,10-diphenyl-9-anthryl radical (**9b**). The ESR signal intensity of **9b** increased reversibly with increasing temperature, thus indicating the onset of the equilibrium with its dimer.

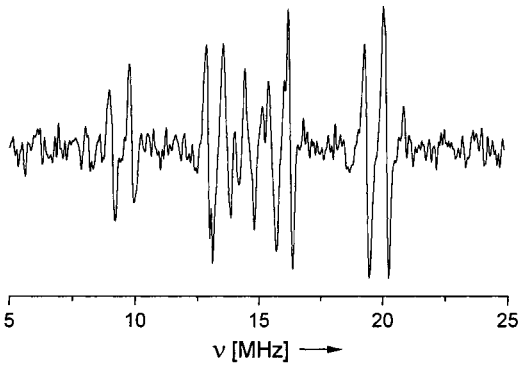

Figure 5. ENDOR spectrum of the 9-methoxy-10,10-diphenyl-9-anthryl radical (**9b**) in diphenyl ether at 20°C

Table 2. Rate constants at 80°C from the kinetic simulation of Scheme 7

$k_{meso\text{-}1c,2c}$ [s^{-1}]	$k_{2c,meso\text{-}1c}$ [s^{-1}]	$k_{2c,rac\text{-}1c}$ [s^{-1}]	$k_{rac\text{-}1c,2c}$ [s^{-1}]	$k_{2c,6a}$ [s^{-1}]	$k_{6a,9a}$ [M^{-1}s^{-1}]	$k_{9a,anti\text{-}8a}$ [M^{-1}s^{-1}]	$k_{9a,syn\text{-}8a}$ [M^{-1}s^{-1}]	$k_{6a,7a}$ [s^{-1}]
1.7·10^{-3}	4.0	3.0	2.6·10^{-4}	0.75	1.6	7.0·10^8	8.0·10^7	3.0·10^{-4}

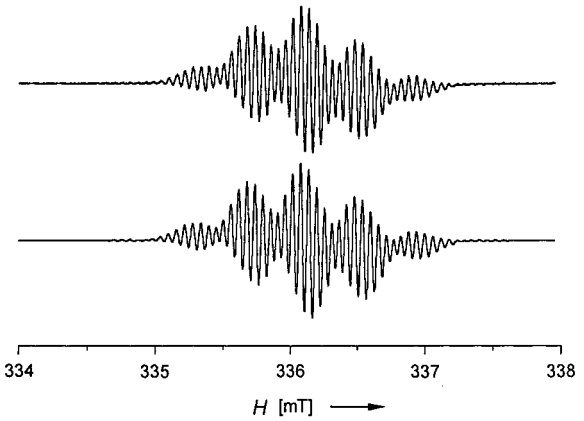

Figure 6. ESR spectrum of the 9-methoxy-10,10-diphenyl-9-anthryl radical (**9b**) in acetonitrile at 20°C. Top: experimental; bottom: simulated

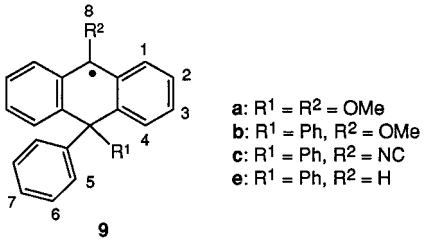

Table 3. ESR parameters of substituted 9-anthryl radicals

	9a[a]	**9b**[b]	**9c**[b]	**9e**[c]
T [°C]	150	20	16	72
g factor	2.0025	2.00255	2.00255	2.00250
hfs [mT] $a(H^1)$	0.34 (2 H)	0.341 (2 H)	0.345 (2 H)	0.334 (2 H)
$a(H^2)$	0.12 (2 H)	0.117 (2 H)	0.120 (2 H)	0.124 (2 H)
$a(H^3)$	0.39 (2 H)	0.398 (2 H)	0.400 (2 H)	0.401 (2 H)
$a(H^4)$	0.12 (2 H)	0.114 (2 H)	0.114 (2 H)	0.111 (2 H)
$a(H^5)$	n. a.[d]	0.057 (4 H)	0.060 (4 H)	0.060 (4 H)
$a(H^6)$	n. a.	0.006 (4 H)	0.006 (4 H)	0.006 (4 H)
$a(H^7)$	n. a.	0.014 (2 H)	0.007 (2 H)	0.012 (2 H)
$a(H^8)$	n. a.	0.074 (3 H)	–	1.362 (1 H)
a(other)	–	1.040 (1 ^{13}C)	0.034 (1 N)	–

[a] In diphenyl ether. – [b] In acetonitrile. – [c] In benzene. – [d] Not analyzed.

7-Methyl-7,8,8-triphenylbenzocyclobutene (1f)

Photolysis of 1-methyl-1,3,3-triphenylindan-2-one (**3f**) in benzene solution at 10°C yielded a mixture of benzocyclobutene **1f** and the styrene derivative **5b**, in slightly variable relative yields depending on the duration of the photolysis.[6] For instance, the **1f/5b** ratio changed from about 57:43 after 2 h (14% conversion of **3f**) to 68:32 after 8 h of photolysis (72% conversion). Clearly, some degree of photochemically-induced 1,5-hydrogen shift occurs in this case, in contrast to **3d**, which gave **1d** as the only detectable photoproduct. By monitoring the process spectrometrically by ^{1}H-NMR, **1f** was found to decay with a rate constant of $k(\mathbf{1f})^{293} = (4.2 \pm 0.1) \times 10^{-4}$ s^{-1} at 20°C, to give mainly **5b**. The slightly lower rate of formation of the latter, $k(\mathbf{5b})^{295} = (3.8 \pm 0.6) \times 10^{-4}$ s^{-1}, indicates a contribution from a minor, additional decay path for **1f**. This was corroborated by the observation of the development, at the same rate, of a UV/vis absorption at $\lambda_{max} = 388$ nm (Figure 7), attributable to 9,10-diphenyl-10-methyl-4*a*,10-dihydroanthracene (**6d**) (α-phenylstyrenes can be ruled out from being responsible for this absorption[17]). The assignment was supported by the detection of corresponding, transient ^{1}H-NMR signals, all exhibiting the same time dependence as the UV/vis absorption [$k(\mathbf{6d})^{296} = (4.9 \pm 0.2) \times 10^{-4}$ s^{-1}]. Two singlets at δ = 1.66 and 1.75, assigned to the diastereomeric 10-methyl groups, pointed to a maximum concentration of **6d** of ca. 11 mol% (relative to **1f**) and a diastereomeric ratio of about 2.6:1, similar to the value found for **6a** (see above). A further transformation of **6d** was not observed within three days.

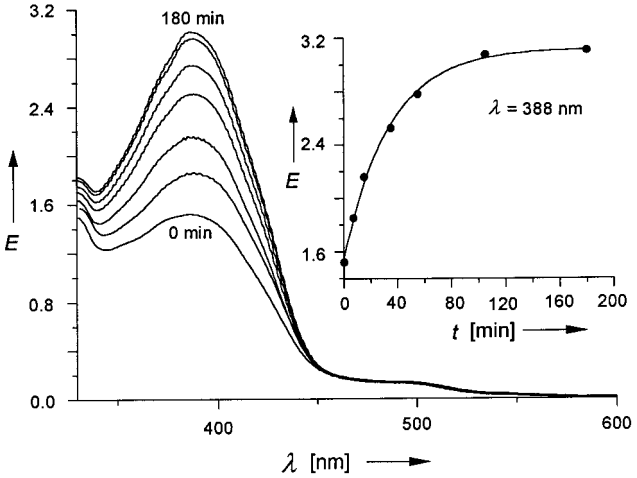

Figure 7. Time-dependent UV/vis spectra of the photolysate of **3f** at 23°C

7-Isocyano-7,8,8-triphenylbenzocyclobutene (1g)

300-nm photolysis of ketone **3g** in [D_3]acetonitrile for 24 h at −30°C afforded benzocyclobutene **1g** in high yield (Figures 8a, b). Heating of the photolysate to 20°C for 30 min resulted in almost complete conversion of **1g** to 10-isocyano-9,10-diphenyl-4a,10-dihydroanthracene (**6e**) (Scheme 3), as indicated by characteristic ^{1}H-NMR resonances in the δ = 4.5−6.5 region (Figure 8c). The assignment of these resonances to **6e** and not to the possible regioisomer **6f** follows from the observation that at 20°C the olefinic signals underwent further decay within 3 d to yield an NMR spectrum exhibiting only minor non-aromatic ^{1}H signals (Figure 8d). 9,10-Diphenylanthracene (**7b**) was identified as the major product (68% isolated yield). Its formation can reasonably be explained in terms of the facile elimination of hydrocyanic acid from **6e**, as confirmed by a peak corresponding to HCN at δ = 4.47 (Figure 8d).

Obviously, the alternative cyclization **2g** → **6f** also took place, albeit to a much lesser extent, as during the decay of **1g** a fairly persistent ESR spectrum (Figure 9) was observed which could be satisfactorily simulated only with a set of hyperfine splittings that matched the 9-isocyano-10,10-di-

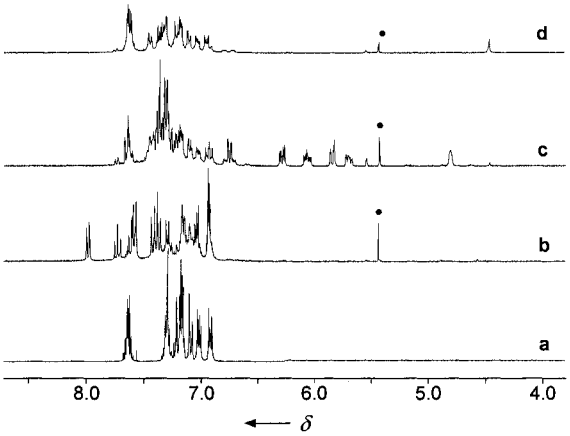

Figure 8. 300-MHz ^{1}H-NMR spectra in [D_3]acetonitrile of (a) ketone **3g** prior to photolysis, (b) after 24 h of photolysis at −30°C, (c) after 30 min. at 20°C, (d) after 3 d at 20°C; (•): unknown photolysis product

phenyl-9-anthryl radical (**9c**) (Table 1). The location of the radical center in **9c** requires **6f** as its precursor. A tiny ^{1}H-NMR peak at δ = 5.55 (Figures 8c, d) is indeed consistent with the 9-hydrogen of the expected 9,10-dihydroanthracene product **8d**, although no definite identification was possible. The ESR spectrum revealed a slight asymmetry, which might be due to a contribution from a second, similar radical, most reasonably **9d** derived from retrodisproportionation of **6e**.

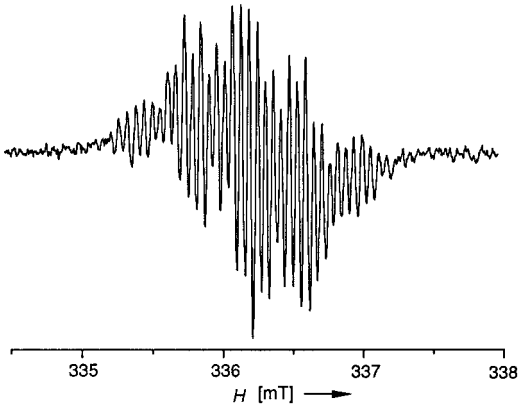

Figure 9. ESR spectrum ([D_3]acetonitrile, 16°C) of **9c**

7,7,8-Triphenylbenzocyclobutene (1h)

The rearrangement of this compound has been investigated previously.[8h] In accordance with the expected lower steric strain in the cyclobutene moiety of **1h**, no change of its ^{1}H-NMR spectrum in [D_6]benzene solution could be detected at temperatures up to 50°C. Above this temperature, a small increase in UV/vis absorption in the λ = 340−395 nm range was observed, attributable to the formation of the corresponding 4a,10-dihydroanthracene derivatives **6g** and/or **6h**.[8h] Retrodisproportionation of the former was indicated by the observation of a weak ESR spectrum (Figure 10), unequivocally identified as being due to radical **9e** by the characteristic α-H doublet splitting of 1.36 mT (Table 3).

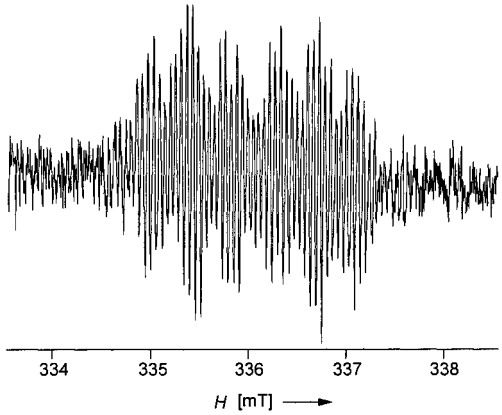

Figure 10. ESR spectrum (benzene, 72°C) of **9e**

Discussion

meso/*rac* Isomerization of 1c

To the best of our knowledge, **1c** is the first benzocyclobutene for which a *meso*/*rac* isomerization process has been investigated at ambient temperature. The considerable steric strain in the cyclobutene moiety, which should be the primary reason for the low barrier to isomerization, is indicated by the experimental C7−C8 bond length (Figure 1) of $d(C7-C8)_{exp}$ = 164.7 pm, which is about 7.1 pm longer than that in unsubstituted benzocyclobutene[18a] and 6.3 pm shorter than the corresponding distance in the more sterically crowded 3,8-dichloro-1,1,2,2-tetraphenylcyclobuta[*b*]naphthalene.[18b] The orientation of the phenyl and methoxy substituents in the solid state is largely reproduced by the PM3-calculated[19] structure, with the one exception that in the calculated structure the methoxy group at C8 has a similar orientation as that at C7. The PM3-calculated bond length of $d(C7-C8)_{calcd}$ = 166.3 pm also compares well with the X-ray value.

The preference for *rac*-**1c** by 4.9 kJ·mol^{-1} (see above) over the *meso* isomer is in agreement with the PM3 calculations, which favor *rac*-**1c** [$\Delta_fH°$(*rac*-**1c**) = 167.8, $\Delta_fH°$(*meso*-**1c**) = 173.2 kJ·mol^{-1}] by about 5.4 kJ·mol^{-1}. The PM3 structures of the three configurational isomers of *o*-quinodimethane **2c** reveal a pronounced distortion of the π-system, with out-of-plane torsional angles of the exocyclic double bonds of 50.8, 53.9, and 57.9° for (*E,E*)-, (*E,Z*)-, and (*Z,Z*)-**2c**, respectively. The calculated heats of formation [$\Delta_fH°$(*E,E*-**2c**) = 181.2, $\Delta_fH°$(*E,Z*-**2c**) = 187.9, $\Delta_fH°$(*Z,Z*-**2c**) = 192.9 kJ·mol^{-1}] increase in the same order.

The data presented here and in our previous paper[6] suggest that only two of the three possible configurational isomers of **2c** are likely to be involved in the thermal isomerization process. Two transients, with lifetimes of τ = 0.16 and 24 μs, observed in the LFP experiments,[6] were originally attributed to (*E,Z*)- and (*Z,Z*)-**2c**. A third, long-lived

(τ = 30 h at 40°C) *o*-quinodimethane species that was produced in the photochemical decomposition of ketone **3c**, but not in the thermal reaction, was reasonably attributed to (*E,E*)-**2c**. Thus, in the discussion of the energetics of the thermal isomerization processes, the involvement of (*E,E*)-**2c** can be disregarded.

Like the benzocyclobutenes **1a**, **1b**,[5] compounds **1c** represent another test case for probing the energetics of "symmetry-forbidden" electrocyclic ring-opening reactions. The barrier for the symmetry-allowed reaction may be evaluated from the racemization kinetics of enantiomerically pure **1c**, e.g. by the GLC method of Roth and co-workers.[5] Unfortunately, our synthetic procedure[6] yielded mainly *meso*-**1c**; attempts to separate the enantiomers from the small fraction of racemic **1c** were not successful.

For the "symmetry-forbidden" *meso*/*rac* isomerization process, three pathways may be envisaged (Scheme 8): (i) a true disrotatory (concerted) one; (ii) a non-concerted, single-bond rotation involving either a biradicaloid transition state or an orthogonal biradical intermediate of type **13**, or (iii) isomerization of the intermediate *o*-quinodimethanes by double-bond rotation.

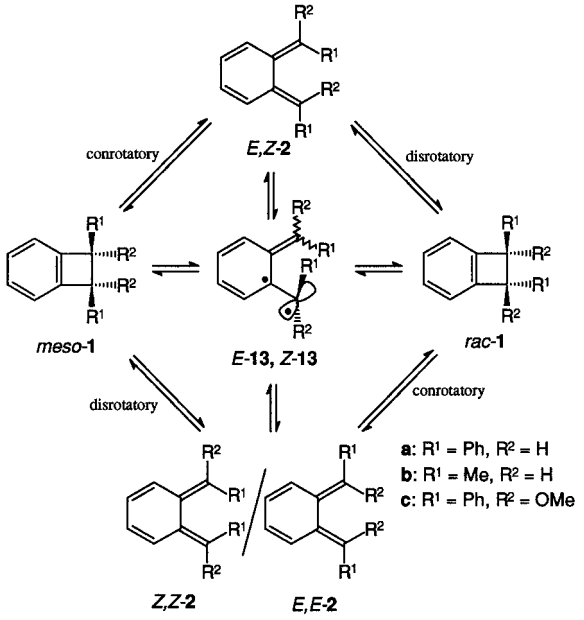

Scheme 8. Possible pathways of *meso*/*rac* isomerization of benzocyclobutenes

Roth[5] provided evidence that for **1a** and **1b** double-bond isomerization of the corresponding *o*-quinodimethanes is unlikely. It was suggested that the system avoids the energetically unfavourable disrotatory pathway by following the biradical one (which does not rely on orbital symmetry considerations). A difficulty then arises in that **13** would thus represent a common transition state for two independent processes, (*E,Z*)-**2** → (*Z,Z*)-**2** and *meso*-**1** → *rac*-**1**, an obvious contradiction to the definition of the transition state. Roth et al. circumvented this problem by arguing that the biradical structure derived from the (*E,Z*)-**2** → (*Z,Z*)-**2** process is not necessarily a transition state, but rather could be an intermediate. **13** would then represent a common intermediate of the (*E,Z*)-**2** → (*Z,Z*)-**2** and *meso*-**1** → *rac*-**1** reactions. In conclusion, in terms of kinetic representation, Scheme 4b rather than Scheme 4a (framed areas) should hold.

For the **1b/2b** couple, a difference of 20.5 kJ·mol^{-1} between the activation barriers for the "forbidden" and the conrotatory isomerization was estimated.[5] This difference dropped to just 4.2 kJ·mol^{-1} in the case of 7,8-diphenylbenzocyclobutene (**1a**), an effect attributed to the higher (benzyl-type) stabilization in the orthogonal biradical transition state/intermediate **13b**. Following this argument, we can assume that for our **1c/2c** system the energy difference between the conrotatory and the "forbidden" process should be of the same order, probably even more in favor of the "forbidden" one due to the additional stabilizing effect of the methoxy groups. Thus, the energetic difference between the "allowed" and "forbidden" reaction pathways might have virtually vanished.

According to our kinetic simulations (Scheme 4b), the rate constants at 20°C for ring-opening of **1c** (Table 1) appear to be only slightly higher than those for diphenyl-*o*-quinodimethane **1a**. For the con- and disrotatory reactions we obtained rate constants of $k_{meso\text{-}\mathbf{1c},EZ\text{-}\mathbf{2c}} = 1.4\cdot10^{-6}$ s^{-1} and $k_{meso\text{-}\mathbf{1c},ZZ\text{-}\mathbf{2c}} = 2.8\cdot10^{-7}$ s^{-1}, respectively. These data have to be compared with the values for **1b**, $k_{meso\text{-}\mathbf{1b},EZ\text{-}\mathbf{2b}} = 9.0\cdot10^{-7}$ s^{-1} and $k_{meso\text{-}\mathbf{1b},ZZ\text{-}\mathbf{2b}} = 1.0\cdot10^{-7}$ s^{-1}, as calculated from Huisgen's[3a] and Roth's[5] activation data. Hence, replacement of the two hydrogen atoms in **1a** by methoxy groups does not seem to exert a noticeable effect on the barriers for ring-opening.

Because the experimental barrier for the conrotatory ring-opening reaction was not available, we attempted to estimate the energy profile of the *meso*/*rac* isomerization processes by semiempirical PM3 calculations. The calculations predict the *o*-quinodimethanes to be 13−25 kJ·mol^{-1} higher in energy than the benzocyclobutenes (Figure 11, bold bars), in line with the experimental data for **1b**.[5] In accord with the experimental evidence, the (*E,E*)-isomer represents the lowest-energy structure of **2c**. Unfortunately, attempts to locate possible transition states as well as singlet biradical intermediates **13** failed due to convergence problems.

Estimates of the activation barriers for ring-opening/ring-closure were therefore sought as follows: By assuming a reasonable *A*-factor of 10^{13} s^{-1} for ring-opening/-closure of *o*-quinodimethanes,[3a,5] from the lifetimes of the two transient species observed by LFP (see above) we calculated activation barriers of E_A(*Z,Z*-**2c** → **1c**) = 34.8 and E_A(*E,Z*-**2c** → **1c**) = 47.0 kJ·mol^{-1}. However, the LFP-derived rate constants were much too high to reproduce the concentration/time profiles shown in Figures 2, 3, and 4 by kinetic simulation. Therefore, the energy barriers displayed in Figure 11 were calculated from the rate constants obtained from the simulation of Scheme 4b (Table 1) using the same *A*-factor. Specifically, barriers for the "allowed" and "forbidden" ring-opening of *meso*-**1c**, E_A(*meso*-**1c** → *E,Z*-**2c**) = 103 and E_A(*meso*-**1c** → *Z,Z*-**2c**) = 107 kJmol^{-1}, were obtained. The corresponding barriers for ring-closure were es-

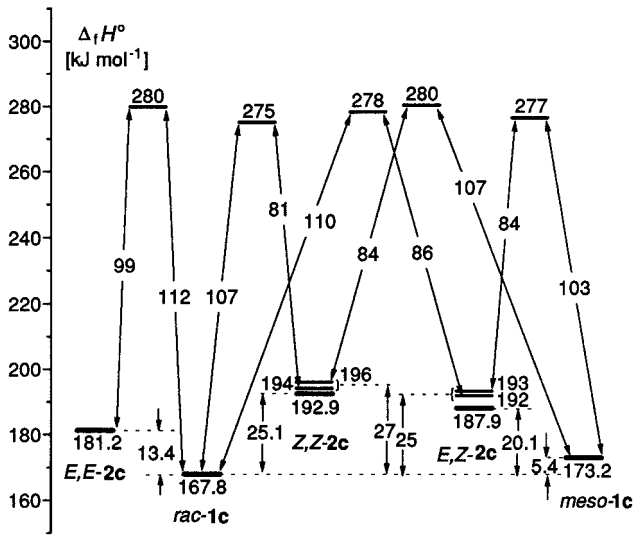

Figure 11. Estimated energy profile of the **1c/2c** system. Bold bars: PM3 data; small bars: data estimated from kinetic simulation, assuming $A = 10^{13}$ s^{-1} (rounded to next decimal number)

timated to be in the range 81−86 kJ·mol^{-1}. Thus, there is an obvious discrepancy between the latter and the LFP-derived barriers. Because the values from the *meso*/*rac* isomerization experiments are in much better accord with the literature data for **1b**,[3a,5] this discrepancy may indicate that our previous assignments of the two transient LFP absorptions were in error, i.e. other species might actually have been the source of the detected absorptions.

In conclusion, the energy profile of the dimethoxy-diphenyl system **1c/2c** appears to be very similar to that of the **1b/2b** system. In particular, the difference between the "allowed" and "forbidden" electrocyclic processes is very small, of the order of 4 kJ·mol^{-1}.

Electrocyclic Hexatriene → Cyclohexadiene Ring-Closure

The formation of dihydroanthracenes **6** in the thermal decay of phenyl-substituted benzocyclobutenes has been reported previously.[8d,8h,20] This reaction can easily be understood as a symmetry-allowed [$_\pi2_s$ + $_\pi2_s$ + $_\pi2_s$] electrocyclic ring-closure of the stereoisomers of the intermediate *o*-quinodimethanes **2** that have at least one of the phenyl substituents in (*Z*)-orientation (Scheme 3).

For the **1c/2c** system, the kinetic simulation according to Scheme 7 (Figure 4, Table 2) predicts that at 80 °C the cyclization of **2c** is about 440 times faster than the ring-opening of **1c**. Assuming again identical *A*-factors of 10^{13} s^{-1} for all the processes, we arrive at a barrier of about 93.7 kJ·mol^{-1} for the **2c** → **6a** transformation, i.e. 8−13 kJ·mol^{-1} higher than the estimated barriers for the **2c** → **1c** ring-closure reactions (Figure 11). This result is in line with the fact that at room temperature no formation of **6a** could be detected by conventional ^{1}H-NMR spectrometry. According to PM3 calculations, the **1c** → **6a** reaction [$\Delta_fH°$(**6a**) = 31.9 kJ·mol^{-1}] is exothermic by about 33−42 kJ·mol^{-1}, i.e. the release of ring strain in **1c** overcompensates for the loss of aromaticity in one phenyl group.

For the **1e/2e** couple, the facile formation of **6b** and **6c** at 30 °C may reflect both a higher steric strain in benzocyclobutene **1e**, as well as an increased tendency of **2e** to undergo the hexatriene ring-closure. From its rate of decay [k(**1e**)^{303} = 3.1·10^{-5} s^{-1}], a barrier of 101.7 kJ·mol^{-1} was estimated for the ring-opening of **1e**, i.e. about 4−8 kJ·mol^{-1} lower than that for **1c**. PM3 calculations predict a negligibly small energy difference between **1e** [$\Delta_fH°$(**1e**) = 446.0 kJ·mol^{-1}] and the two configurations of the *o*-quinodimethanes **2e** [$\Delta_fH°$(*E,Z*-**2e**) = 447.3; $\Delta_fH°$(*Z,Z*-**2e**) = 451.9 kJ·mol^{-1}]. As no noticeable build-up of **2e** could be detected, the further electrocyclic ring-closure appears to be accelerated [k(**6b** + **6c**)^{303} = 3.1·10^{-5} s^{-1}] compared to that in the case of **1c**. This is in line with increased reaction enthalpies for the **1e** → **6b** and **1e** → **6c** conversions, calculated to be about −39 and −58 kJ·mol^{-1}, respectively.

According to PM3 calculations, for the triphenyl-methyl system **1f/2f** the relative energies of the benzocyclobutene **1f** [$\Delta_fH°$(**1f**) = 560.2 kJ·mol^{-1}] and the *o*-quinodimethanes **2f** [$\Delta_fH°$(*E,Z*-**2f**) = 559.7; $\Delta_fH°$(*Z,Z*-**2f**) = 569.9 kJ·mol^{-1}] are very similar to those of the **1e/2e** couple. Compound **2f** appears to be more reactive in the [$_\pi2_s$ + $_\pi2_s$ + $_\pi2_s$] electrocyclic process than the triphenyl-methoxy analogue **2e**, as indicated by the faster rate of development [k(**6d**)^{296} = (4.9 ± 0.2) ×10^{-4} s^{-1}] of the corresponding UV/vis absorption (Figure 7). Only methyl group resonances due to the two diastereomers of **6d** were detected in the ^{1}H-NMR spectra, hence ring-closure of **2f** seems to occur almost exclusively across the (*Z*)-oriented phenyl group at the diphenyl-substituted double bond, and does not involve the one at the phenyl-methyl site. This is in contrast to the situation in **2e**, where ring-closure proceeds into both directions. Rapid decay upon reaction with NO[6] identified the additional weak absorption in the 450−550 nm range of the UV/vis spectrum of the photolysate of **3f** (Figure 7) as being due to a rather long-lived *o*-quinodimethane. However, as no temporal change of this absorption was monitored in the time window of the decay of **1f**, it must be attributed to a configuration of **2f**, most reasonably (*Z,Z*)-**2f**, that is only photochemically accessible and is not involved in the thermal processes.

In terms of cyclobutene ring-opening and [$_\pi2_s$ + $_\pi2_s$ + $_\pi2_s$] ring-closure, the most reactive system among those investigated here is the **1g/2g** couple. The NMR spectra (Figures 8b, 8c) reveal a preferred, by at least a factor of ten, formation of **6e** over **6f**, with a rate constant ≥ 10^{-3} s^{-1} at ambient temperature. Since no noticeable build-up of *o*-quinodimethanes **2g** could be monitored, this rate constant should reflect the ring-opening of **1g**. Also, the **2g** → **6e** ring-closure should be faster. As **6e** can only be formed from the (*E,Z*)-configuration of **2g**, one may conclude that ring-opening of **1g** proceeds preferably by an "inward" rotation of the isocyano group. Intuitively, such a rotation can be expected to be stereochemically favoured, though PM3 calculations predict similar thermal stabilities for (*E,Z*)-**2g** ($\Delta_fH°$ = 865.7 kJ·mol^{-1}) and (*Z,Z*)-**2g** ($\Delta_fH°$ = 867.1

kJ·mol^{-1}). The heat of formation of the parent benzocyclobutene **1g** ($\Delta_fH°$ = 869.3 kJ·mol^{-1}) is predicted to be slightly higher, in agreement with the "fast" rate of decay of this species. It should be noted that only one diastereomer of **6e** could be detected in the ^{1}H-NMR spectra (Figure 8c). We explain this fact in terms of a faster elimination of HCN from one of the diastereomers rather than by invoking a highly diastereoselective ring-closure of (*E,Z*)-**2g**, since a significant amount of 9,10-diphenylanthracene (**7b**) was already present after a reaction period of just 30 min (Figure 8c).

1,5-H Shift Reactions

Similar to the situation seen with **1c**, the PM3 calculations predict the thermal stability of *rac*-**1d** ($\Delta_fH°$ = 401.2 kJ·mol^{-1}) to be 4.6 kJ·mol^{-1} higher than that of its *meso* isomer ($\Delta_fH°$ = 405.8 kJ·mol^{-1}). The three configurational isomers of the *o*-quinodimethanes **2d** [$\Delta_fH°$(*E,E*-**2d**) = 408.8; $\Delta_fH°$(*E,Z*-**2d**) = 412.5; $\Delta_fH°$(*Z,Z*-**2d**) = 420.5 kJ·mol^{-1}] are calculated to be higher in energy by 7.6, 11.3, and 19.3 kJ·mol^{-1}, respectively, i.e. following the same order as in the case of **2c**. On steric grounds, **1d** was expected to exhibit reactivity similar to that of **1c**. However, the lack of any product formation at room temperature points to a somewhat higher barrier for ring-opening in this case. At elevated temperature, ring-opening is indicated by formation1 of the 1,5-H shift product **5a**, with the steady-state level of *o*-quinodimethanes **2d** below the ^{1}H-NMR detection limit. To what extent the observed change of the *meso*/*rac* ratio from 1:1.2 to 1:3 over the reaction period of 26 h at 60°C reflects the setting-up of a possible *meso*/*rac* equilibrium and/or the relative reactivity of the (*E,E*)- and (*E,Z*)-diastereomers of **2d** in the 1,5-H shift reaction cannot be determined. In any case, the failure to detect dihydroanthracene or anthracene products implies that for (*E,Z*)-**2d** the rate of the 1,5-H shift reaction overrules that of a possible hexatriene → cyclohexadiene ring-closure by at least a factor of ten, and/or that (*Z,Z*)-**2d** is too high in energy to play a significant role as an intermediate.

For the triphenyl-methyl system **1f/2f**, the 1,5-H shift reaction **2f** → **5b** is statistically less favoured, though still the dominant reaction, overruling the **2f** → **6d** ring-closure reaction (see above) by about a factor of nine, as deduced from the relative intensities of the appropriate ^{1}H-NMR resonances. As a 1,5-H shift can only occur from the (*E,Z*)-configuration, the extensive conversion of **1f** to **5b** indicates that ring-opening of **1f** produces primarily (*E,Z*)-**2f**. This is in agreement with the PM3 results (see above), which place (*Z,Z*)-**2f** about 10.2 kJ·mol^{-1} above (*E,Z*)-**2f**.

Retrodisproportionation

Rüchardt et al.[16] have recently reviewed a class of uncatalyzed, bimolecular hydrogen-transfer reactions that are initiated by a hydrogen atom transfer from a σ-type C−H hydrogen donor to a π-type hydrogen acceptor. Rüchardt and co-workers provided evidence that the so-called "retrodisproportionation" reaction involves homolytic C−H bond cleavage, thereby producing a pair of carbon-centered radicals, rather than following concerted hydrogen-transfer pathways. Obviously, such a reaction is also responsible for the conversion of 4a,10-dihydroanthracenes **6** to the corresponding 9,10-dihydroanthracenes **8** (a monomolecular **6** → **8** transformation involving a concerted 1,3-H shift would be a symmetry-forbidden reaction). The **6** → **8** conversions (Scheme 9) represent examples of a variant of the retrodisproportionation process, where a single substrate acts as both a hydrogen donor and as a hydrogen acceptor. The driving force for the overall process is most certainly the gain in aromatic stabilization. ESR detection of the 9-anthryl radicals **9** provides sound evidence that the reaction indeed involves initial homolytic cleavage of the 4*a*-C−H bond (Scheme 9, reaction 1). This would result in cyclohexadienyl- and/or benzyl-type radicals **12** and/or **14** being generated concomitantly. Whereas radicals **12** are certainly too short-lived to be observed under the conditions employed (their dimerization is sterically unhindered), radicals **9** and **14** are expected (proven for **9b**) to be in equilibrium with their dimers and co-dimers. The high yields of 9,10-dihydroanthracenes **8a−c** implies that further back-transfer of hydrogen (disproportionation) occurs between radicals **9** and **12** and/or **14**, ultimately leading to the conversion of all **6** into **8** (Scheme 9, reactions 2−4). Alternatively, formation of **8** may also be explained in terms of direct hydrogen atom transfer from **6** to **9**. As radicals **9** are regenerated in this step, a chain reaction would be initiated (Scheme 9, reaction 5).

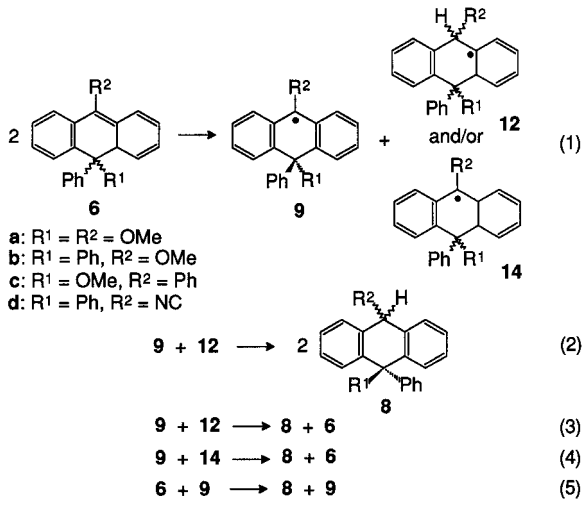

Scheme 9. 9,10-Dihydroanthracenes via retrodisproportionation of 4a,10-dihydroanthracenes

Our analytical and kinetic data do not allow an unambiguous discrimination between the two possibilities. However, trial kinetic simulations of the concentration-time dependencies in Figure 4 reveal that in the case of such a chain process the maximum concentration of the intermediate dihydroanthracenes **6a** should be of the order of just 10^{-5} M. The much higher, ^{1}H-NMR-detectable yield of **6a**

is only satisfactorily reproduced if at least one of the disproportionation reactions **9** + **12** or **9** + **14** is explicitly considered. By-products, which may have resulted from possible coupling reactions of radicals **8**, **9**, **12**, and **14**, were sometimes detected in the ^{1}H-NMR spectra, but their yields were far too low for reliable identification.

The extent to which retrodisproportionation can occur in our systems depends on the competition with the possible elimination of R^{1}H from the 4a,10-dihydroanthracenes to give 9,10-disubstituted anthracenes **7**. Thus, whereas benzene elimination from **6b** is highly unfavourable and methanol elimination from **6a** and **6c** can only compete to some degree, the retrodisproportionation decay path plays only a minor role in the case of **6e** due to the rapid elimination of HCN. The mechanism of elimination of methanol and hydrocyanic acid from **6a/6c** and **6e**, respectively, was not further explored. It might involve ionic, proton-catalyzed reactions as traces of water were invariably present in our solutions.

Experimental Section

General Remarks: ^{1}H- and ^{13}C-NMR spectra: Varian Gemini-200 and Bruker AMX-300. Internal standard TMS. − IR: Perkin-Elmer 1600 series FT-IR. − UV/vis: Varian Cary 219, modified for use with light pipes and thermostatted sample holders. − GC/MS: Hewlett-Packard HP 5971A mass-sensitive detector (70 eV) and HP5890 GC, capillary column HP 1; 50 m × 0.2 mm; SF 0.33 μm. − High-resolution MS: Fisons Instruments VG Pro Spec 300 (70 eV). − HPLC: Varian LC 5000 and Hewlett-Packard 1040 diode-array UV detector, Varian MCH-10 column (10 μm; 4 × 300 mm). − ESR: Bruker ER-420 X-band spectrometer (9.4 GHz) equipped with a double cavity and a variable temperature unit. − ESR data acquisition: Pentium PC equipped with a Microstar DAP 1200/4 data acquisition board and DigiS (GfS Aachen, Germany) software. − ENDOR: Bruker ESP-300 − Melting points (uncorrected): Büchi 510.

Materials: The synthesis of ketones **3c**−**h** and **3j** has been described previously.[6] 1-Isocyano-1,3,3-triphenylindan-2-one (**3i**) was synthesized from 1,3,3-triphenylindan-2-one (**3j**) via 1-bromo-1,3,3-triphenylindan-2-one.

1-Bromo-1,3,3-triphenylindan-2-one: To 3.0 g (8.32 mmol) of **3i** in tetrachloromethane (60 mL) was added 0.46 mL (8.95 mmol) of bromine and the solution was stirred in the dark for 24 h. The solvent was then evaporated under reduced pressure (1 Pa) to leave 3.55 g (8.08 mmol, 97%) of an orange solid, m.p. 184°C. − ^{1}H NMR (300 MHz, $CDCl_3$): δ = 7.70−6.96 (m). − ^{13}C NMR (75 MHz, BB, $CDCl_3$): δ = 65.2, 67.1, 127.2, 127.3, 127.4, 127.6, 128.2, 128.3, 128.4, 128.8, 128.9, 129.0, 130.4 (s, *tert.* aromatic C), 137.7, 141.1, 141.5, 142.9, 143.1 (s, *quat.* aromatic C), 208.4 (s, C=O). − IR (KBr): $\tilde{\nu}$ = 3050 cm^{-1}, 3032, 1756 (C=O), 1121, 1056, 762, 744, 722, 700.

Isocyano-1,3,3-triphenylindan-2-one (**3i**): Under nitrogen, 1.25 g (9.34 mmol) silver(I) cyanide was added to a solution of 3.0 g (6.83 mmol) 1-bromo-1,3,3-triphenylindan-2-one in DMF (120 mL). After stirring for 24 h in the dark, the solvent was removed in vacuo (1 Pa) and the residue was redissolved in chloroform (100 mL). The resulting solution was washed with sodium cyanide solution (10%; 3 × 50 mL), water (3 × 40 mL), and finally with saturated sodium chloride solution (40 mL). After drying over magnesium sulfate and evaporation of the solvent, the residue was purified by column chromatography on silica gel (30 × 4.5 cm; eluent $CHCl_3$) to give 0.72 g **3i** (1.87 mmol, 28%), colorless solid, m.p. 159−160°C. − ^{1}H NMR (300 MHz, $CDCl_3$): δ = 7.70−6.97 (m). − ^{13}C NMR (75 MHz, BB, $CDCl_3$): δ = 67.4, 72.2, 125.8, 126.6, 127.5 (2 C), 127.6, 128.4, 128.5 (3 C), 128.8, 129.0, 129.6, 131.0 (s, *tert.* aromatic C), 135.5, 136.9, 1139.1, 143.0, 144.1 (s, *quat.* aromatic C), 159.0 (s, NC), 204.8 (s, C=O). − IR (KBr): $\tilde{\nu}$ = 3059 cm^{-1}, 3034, 2128 (NC), 1756 (C=O), 770, 750, 738, 695. − UV/vis (CH_3CN): λ_{max} (log ε) = 314 nm (2.55), 325 (2.54). − MS (70 ev); *m/z* (%): 385 (2) [M$^+$], 356 (100), 331 (24), 280 (52). − HR-MS (70 eV): $C_{28}H_{19}NO$: calcd. 385.1467; found 385.1453.

Photolytic Generation of *o*-Quinodimethanes from Ketones 3a−j: The general procedure for photolytic decarbonylation of 2-indanones and the spectroscopic properties of the products not mentioned in the following have been reported in ref.[6]

Kinetic Measurements: The kinetics of the thermal rearrangements were measured spectrometrically by integration of the non-aromatic ^{1}H-NMR signals, using 1,2,4,5-tetramethylbenzene as internal standard and cross-checking the mass balance against the sum of the methoxy group integrals. Generally, the raw photolysates from the photolytic decarbonylation of deoxygenated 0.05 M solutions of ketones **3** in the above mentioned deuterated solvents were directly employed in sealed NMR tubes, except in the case of **1c**, where purified material was used. Product yields were corrected for conversion of the starting material and photochemically produced by-products. Short-term kinetics were measured by thermostatting (± 0.3°C) the sample in the probe head of the spectrometer; for long-term kinetics the samples were kept in a thermostatted bath (± 0.1°C) in the dark and were only briefly removed for recording the spectra. For the decomposition of **1c** in the presence of oxygen the samples were equilibrated by bubbling with oxygen (5.0) or air, respectively, for 30 min in septum-capped NMR tubes by means of hypodermic needles. The oxygen level in the tubes was maintained by daily flushing the head space with oxygen or air, respectively. Data analysis was performed with the CKS simulation software[9] using the rate constants from single exponential least-squares fits to the respective concentration-time data as starting values.

9,10-Dimethoxy-10-phenyl-4a,10-dihydroanthracene (**6a**) (2 isomers, ratio ca. 2.6:1): Major isomer: ^{1}H NMR (300 MHz, CD_3CN): δ = 3.05 (s, 3 H, OC*H*$_3$), 3.73 (s, 3 H, OC*H*$_3$), 4.42 (br m, 1 H), 5.37−5.41 (m, 1 H), 5.85−5.91 (m, 2 H), 6.59−6.64 (dm, *J* = 10 Hz, 1 H), 6.75 (dm, *J* = 7.9 Hz, 1 H), 6.9−7.7 (m, 8 H). − Minor isomer: ^{1}H NMR (300 MHz, CD_3CN): δ = 3.00 (s, 3 H, OC*H*$_3$), 3.67 (s, 3 H, OC*H*$_3$), 4.85 (br m, 1 H), 5.40−5.42 (m, 1 H), 5.85−5.98 (m, 2 H), 6.50−6.56 (dm, *J* = 10 Hz, 1 H), 6.69 (dm, *J* = 7.9 Hz, 1 H), 6.9−7.7 (m, 8 H).

9-Methoxy-10,10-diphenyl-4a,10-dihydroanthracene (**6b**): ^{1}H NMR (300 MHz, CD_3CN): δ = 3.53 (s, 3 H, OC*H*$_3$), 4.95 (m, 1 H), 5.71 (ddm, *J* = 10, 4 Hz, 1 H), 5.85−5.95 (m, 1 H), 6.08 (ddt, *J* = 10.4, 4.0, 1.2 Hz, 1 H), 6.69 (dm, *J* = 7.8 Hz, 1 H), 6.95−7.7 (m, 13 H).

10-Methoxy-9,10-diphenyl-4a,10-dihydroanthracene (**6c**) (2 isomers): Major isomer: ^{1}H NMR (300 MHz, CD_3CN): δ = 3.34 (s, 3 H, OC*H*$_3$), 4.55 (br m, 1 H), 5.43 (dm, *J* = 10 Hz, 1 H), 5.84−5.95 (m, 2 H), 6.54 (dm, *J* = 10.4 Hz, 1 H), 6.82 (dm, *J* = 7.5 Hz, 1 H), 6.95−7.7 (m, 13 H). − Minor isomer: ^{1}H NMR (300 MHz, CD_3CN): δ = 3.11 (s, 3 H, OC*H*$_3$), 4.88 (br m, 1 H), 5.37 (dm, *J* = 10 Hz, 1 H), 5.73−5.98 (m, 2 H), 6.71 (dm, *J* = 10.4 Hz, 1 H), 6.75 (dm, *J* = 7.5 Hz, 1 H), 6.95−7.7 (m, 13 H).

9,10-Diphenyl-10-methyl-4a,10-dihydroanthracene (**6d**) (2 isomers, ratio ca. 2.6:1): Major isomer: ^{1}H NMR (300 MHz, C_6D_6): δ =

1.67 (s, 3 H, CH_3), 4.02−4.10 (m), 4.43 (m, 1 H), 5.2−5.3 (m), 5.42−5.52 (m), 5.97−6.25 (m). − Minor isomer: ^{1}H NMR (300 MHz, C_6D_6): δ = 1.75 (s, 3 H, CH_3), 4.02−4.10 (m), 4.88 (m, 1 H), 5.2−5.3 (m), 5.42−5.52 (m), 5.97−6.25 (m).

10-Isocyano-9,10-diphenyl-4a,10-dihydroanthracene (**6e**): ^{1}H NMR (300 MHz, CD_3CN): δ = 4.75 (br m, 1 H), 5.65 (dm, *J* = 10 Hz, 1 H), 5.75 (dm, *J* = 10 Hz, 1 H), 6.05 (dm, *J* = 10.4 Hz, 1 H), 6.35 (dm, *J* = 7.5 Hz, 1 H), 6.7 (dm, *J* = 7.5 Hz, 1 H), 6.9−7.7 (m, 13 H).

9-Methoxy-10-phenylanthracene (**7a**):[12a,12b] ^{1}H NMR (300 MHz, CD_3CN): δ = 4.16 (s, 3 H, OCH_3), 7.05−7.65 (m, 11 H), 8.37 (dd, *J* = 8.8, 1 Hz, 2 H). − ^{13}C NMR (75 MHz, DEPT, CD_3CN): δ = 63.9 (s, OCH_3), 123.1, 126.2, 126.7, 127.3 (?), 127.7, 129.5, 132.2 (s, *tert.* aromatic C), 133.9, 139.9, 149.0 (s, *quat.* aromatic C).

9,10-Dimethoxy-10-phenyl-9,10-dihydroanthracene (**8a**) (2 isomers, ratio ca. 9.4:1): Major isomer: ^{1}H NMR (300 MHz, CD_3CN): δ = 2.95 (s, 3 H, OCH_3), 3.00 (s, 3 H, OCH_3), 5.82 (s, 1 H), 7.12−7.25 (m, 4 H), 7.32−7.45 (m, 5 H), 7.50−7.62 (m, 2 H), 7.68−7.73 (dd, *J* = 7.7, 0.8 Hz, 2 H). − ^{13}C NMR (75 MHz, DEPT-135, CD_3CN): δ = 51.9 (s, OCH_3), 52.2 (s, OCH_3), 73.1 (s, *tert.* aliphatic C), 79.9 (s, *quat.* aliphatic C), 126.3, 127.3, 128.4, 128.6, 128.7, 129.0, 129.3 (s, *tert.* aromatic C), 135.5, 135.9, 150.1 (s, *quat.* aromatic C). − Minor isomer: ^{1}H NMR (300 MHz, CD_3CN): δ = 2.74 (s, 3 H, OCH_3), 3.37 (s, 3 H, OCH_3), 5.39 (s, 1 H), 7.12−7.25 (m, 4 H), 7.32-7.45 (m, 5 H), 7.50−7.62 (m, 2 H), 7.68−7.73 (dd, *J* = 7.7, 0.8 Hz, 2 H). − ^{13}C NMR (75 MHz, DEPT-135, CD_3CN): δ = 51.4 (s, OCH_3), 56.1 (s, OCH_3), 77.4 (s, *tert.* aliphatic C), 80.6 (s, *quat.* aliphatic C), 127.2, 127.3, 128.5, 128.5, 128.9, 129.8, 130.4 (s, *tert.* aromatic C), 141.0, 136.1, 153.0 (s, *quat.* aromatic C).

9-Methoxy-10,10-diphenyl-9,10-dihydroanthracene (**8b**): ^{1}H NMR (300 MHz, [D_6]DMSO): δ = 2.74 (s, 3 H, OCH_3), 5.59 (s, 1 H), 7.1−7.7 (m, 18 H).

10-Methoxy-9,10-diphenyl-9,10-dihydroanthracene (**8c**) (2 isomers, ratio ca. 8.5:1): Major isomer: ^{1}H NMR (300 MHz, [D_6]DMSO): δ = 3.07 (tentative) (s, 3 H, OCH_3), 5.53 (s, 1 H), 7.1−7.7 (m, 18 H). − Minor isomer: ^{1}H NMR (300 MHz, [D_6]DMSO): δ = 3.04 (tentative) (s, 3 H, OCH_3), 5.78 (s, 1 H), 7.1−7.7 (m, 18 H).

***rac*-3,6-Dimethoxy-3,6-diphenyl-4-benzo-1,2-dioxane** (*rac*-**10**) (stereochemical assignment tentative): ^{1}H NMR (300 MHz, CD_3CN): δ = 3.57 (s, 3 H, OCH_3), 7.16 (dd, *J* = 6.0, 3.2 Hz, 2 H), 7.32−7.74 (m, 10 H). − ^{13}C NMR (75 MHz, DEPT, CD_3CN): δ = 53.04 (O*C*H$_3$), 104.19 (s, *quat.* aliphatic C), 128.06, 128.20, 129.22, 129.22, 129.98 (s, *tert.* aromatic C), 135.12, 139.0 (s, *quat.* aromatic C).

***meso*-3,6-Dimethoxy-3,6-diphenyl-4-benzo-1,2-dioxane** (*meso*-**10**) (stereochemical assignment tentative): ^{1}H NMR (300 MHz, CD_3CN): δ = 3.38 (s, 3 H, OCH_3), 6.95 (dd, *J* = 6.0, 3.6 Hz, 2 H), 7.32−7.74 (m, 10 H). − ^{13}C NMR (75 MHz, DEPT, CD_3CN): δ = 53.18 (s, O*C*H$_3$), 105.31 (s, *quat.* aliphatic C), 128.10, 128.24, 129.60, 129.51, 130.01 (s, *tert.* aromatic C), 136.08, 140.67 (s, *quat.* aromatic C).

10-Methoxy-10-phenylanthrone (**11**): ^{1}H NMR (300 MHz, CD_3CN): δ = 2.98 (s, 3 H, OCH_3), 7.2−7.7 (m, 11 H), 8.27 (ddd, *J* = 8.1, 1.1, 1.0 Hz, 2 H). − IR (KBr): $\tilde{\nu}$ = 1670 cm^{-1} (C=O)[12].

ESR Measurements: ESR experiments were carried out in deoxygenated solvents in sealed 4-mm o.d. quartz tubes. ESR parameters were refined by computer simulation using the LMB simulation program.[21]

ENDOR Measurements: ENDOR spectra were recorded at 20°C. The samples contained 10^{-2} M solutions of **1c** in deoxygenated diphenyl ether. Microwave power: 8 mW, radiofrequency power: 1 dB, modulation depth: 34 kHz.[22]

Table 4. Bond lengths [Å] for *meso*-**1c**

bond	bond length	bond	bond length
O(1)−C(7)	1.418(2)	C(8)−C(17)	1.504(2)
O(1)−C(9)	1.423(2)	C(11)−C(12)	1.384(3)
O(2)−C(8)	1.416(2)	C(11)−C(16)	1.391(2)
O(2)−C(10)	1.430(2)	C(12)−C(13)	1.386(3)
C(1)−C(6)	1.376(2)	C(13)−C(14)	1.383(3)
C(1)−C(2)	1.393(2)	C(14)−C(15)	1.377(3)
C(1)−C(7)	1.533(2)	C(15)−C(16)	1.384(3)
C(2)−C(3)	1.390(3)	C(17)−C(18)	1.388(2)
C(3)−C(4)	1.399(3)	C(17)−C(22)	1.391(2)
C(4)−C(5)	1.391(2)	C(18)−C(19)	1.386(3)
C(5)−C(6)	1.382(2)	C(19)−C(20)	1.379(3)
C(6)−C(8)	1.525(2)	C(20)−C(21)	1.383(3)
C(7)−C(11)	1.510(2)	C(21)−C(22)	1.376(3)
C(7)−C(8)	1.647(2)		

Table 5. Bond angles [°] for *meso*-**1c**

bond	bond angle	bond	bond angle
C(7)−O(1)−C(9)	113.75(12)	C(17)−C(8)−C(6)	117.74(14)
C(8)−O(2)−C(10)	117.25(12)	O(2)−C(8)−C(7)	115.45(13)
C(6)−C(1)−C(2)	122.2(2)	C(17)−C(8)−C(7)	114.93(12)
C(6)−C(1)−C(7)	94.93(13)	C(6)−C(8)−C(7)	85.07(12)
C(2)−C(1)−C(7)	142.8(2)	C(12)−C(11)−C(16)	118.4(2)
C(3)−C(2)−C(1)	115.3(2)	C(12)−C(11)−C(7)	120.4(2)
C(2)−C(3)−C(4)	122.5(2)	C(16)−C(11)−C(7)	121.2(2)
C(5)−C(4)−C(3)	121.2(2)	C(11)−C(12)−C(13)	120.8(2)
C(6)−C(5)−C(4)	116.1(2)	C(14)−C(13)−C(12)	120.2(2)
C(1)−C(6)−C(5)	122.7(2)	C(15)−C(14)−C(13)	119.6(2)
C(1)−C(6)−C(8)	95.23(13)	C(14)−C(15)−C(16)	120.1(2)
C(5)−C(6)−C(8)	142.1(2)	C(15)−C(16)−C(11)	120.9(2)
O(1)−C(7)−C(11)	111.40(13)	C(18)−C(17)−C(22)	118.7(2)
O(1)−C(7)−C(1)	116.66(12)	C(18)−C(17)−C(8)	122.1(2)
C(11)−C(7)−C(1)	116.90(13)	C(22)−C(17)−C(8)	119.2(2)
O(1)−C(7)−C(8)	107.84(12)	C(19)−C(18)−C(17)	120.2(2)
C(11)−C(7)−C(8)	116.59(13)	C(20)−C(19)−C(18)	120.4(2)
C(1)−C(7)−C(8)	84.75(12)	C(19)−C(20)−C(21)	119.7(2)
O(2)−C(8)−C(17)	105.96(12)	C(22)−C(21)−C(20)	120.0(2)
O(2)−C(8)−C(6)	117.14(13)	C(21)−C(22)−C(17)	121.0(2)

Quantum Chemical Calculations: Semiempirical PM3 calculations[19] were carried out with the SPARTAN 4.0.3 program package (Wavefunction Inc., Irvine) on a Silicon Graphics Indy workstation. Structures were fully optimized with respect to all geometrical coordinates.

Crystal Structure Determination of *meso*-1c: $C_{22}H_{20}O_2$, formula weight 316.38, crystal colour pale yellow, plate-shaped, approximate dimensions 0.67 × 0.52 × 0.29 mm, measured on a Nicolet R3 diffractometer with Mo-K_α radiation. *T* = 120 K. Cell dimensions (from 50 centered reflections): *a* = 8.965(3), *b* = 11.903(3), *c* = 15.874(3) Å, *V* = 1693.8(7) Å^3, orthorhombic crystal system, *Z* = 4, $d_{calcd.}$ = 1.241 g·cm^{-3}, μ = 0.078 mm^{-1}, space group $P2_12_12_1$, data collection of 4413 intensities ($2\Theta_{max}$ = 50°), 2909 independent (R_{merg} = 0.0323), no absorption or extinction correction, structure solution with direct methods (SHELXS-86) and refinement on F^2 (Siemens SHELXTL Vers. 5.03), 217 parameters, the hydrogen atom positions were calculated and refined as riding groups with the 1.2 fold (1.5 fold for methyl groups) isotropic *U* value of the corresponding C atoms. *R1* = 0.0406 [2762 observed data with $F_o \geq 4\sigma(F)$], w*R*2 (all data) = 0.0982, Go*F* = 1.066, $w^{-1} = \sigma^2(F_o^2) + (0.0656 \cdot P)^2 + (0.2334 \cdot P)$, where $P = [(\max F_o^2)$

+ (2 F_c^2)]/3, maximum residual electron density 0.176 eÅ^{-3}, absolute structure parameter 0.2(12). Crystallographic data (excluding structure factors) for the structure reported in this paper have been deposited with the Cambridge Crystallographic Data Centre as supplementary publication no. CCDC-101797. Copies of the data can be obtained free of charge on application to CCDC, 12 Union Road, Cambridge CB2 1EZ, U.K. [Fax: (internat.) +44 (0)1223/336033; E-mail: deposit@ccdc.cam.ac.uk].

Acknowledgments

This work was supported by the Deutsche Forschungsgemeinschaft.

[1] [1a] J. J. McCullogh, *Acc. Chem. Res.* **1980**, *13*, 270−276. − [1b] C. W. G. Fishwick, D. W. Jones in *The Chemistry of Quinoid Compounds, Vol. 2* (Eds.: S. Patai, Z. Rappoport), Wiley, Chichester, **1988**, pp. 403−453. − [1c] J. L. Charlton, M. M. Alauddin, *Tetrahedron* **1987**, *43*, 2873−2889.

[2] R. B. Woodward, R. Hoffmann, *Die Erhaltung der Orbitalsymmetrie*, Akademische Verlagsgesellschaft Geest & Portig, Leipzig, **1970**, p. 50; *cf. Angew. Chem*. **1969**, *81*, 797−869; *Angew. Chem. Int. Ed. Engl.* **1969**, *8*, 781.

[3] [3a] R. Huisgen, H. Seidel, *Tetrahedron Lett.* **1964**, 3381−3384. − [3b] G. Quinkert, K. Opitz, W. W. Wiersdorff, M. Finke, *Tetrahedron Lett.* **1965**, 3009−3013.

[4] L. A. Carpino, *J. Am. Chem. Soc*. **1962**, *84*, 2196−2201.

[5] W. R. Roth, V. Rekowski, S. Börner, M. Quast, *Liebigs Ann.* **1996**, 409−430.

[6] T. Paul, M. A. Hassan,. D. V. Avila, H.-G. Korth, R. Sustmann, *J. Org. Chem.* **1996**, *61*, 6835−6848.

[7] [7a] H.-G. Korth, K. U. Ingold, R. Sustmann, H. de Groot, H. Sies, *Angew. Chem*. **1992**, *107*, 915−917; *Angew. Chem. Int. Ed. Engl.* **1992**, *31*, 891−893. − [7b] H.-G. Korth, R. Sustmann, P. Lommes, T. Paul, A. Ernst, H. de Groot, L. Hughes, K. U. Ingold, *J. Am. Chem. Soc*. **1994**, *116*, 2767−2777.

[8] [8a] G. Quinkert, *Pure Appl. Chem.* **1964**, *9*, 607−621. − [8b] K. H. Grellmann, J. Palmowski, G. Quinkert, *Angew. Chem*. **1971**, *83*, 209−210; *Angew. Chem. Int. Ed. Engl.* **1971**, *10*, 196−197. − [8c] G. Quinkert, J. Palmowski, H. P. Lorenz, W. W. Wiersdorff, M. Finke, *Angew. Chem*. **1971**, *83*, 210−212; *Angew. Chem. Int. Ed. Engl.* **1971**, *10*, 197−198. − [8d] G. Quinkert, W. W. Wiersdorff, M. Finke, K. Opitz, F.-G. von der Haar, *Chem. Ber.* **1968**, *101*, 2302−2325. − [8e] K. K. de Fonseka, J. J. McCullough, A. J. Yarwood, *J. Am. Chem. Soc*. **1979**, *101*, 3277−3282. − [8f] V. Wintgens, J. C. Netto-Ferreira, H. L. Casal, J. C. Scaiano, *J. Am. Chem. Soc*. **1990**, *112*, 2363−2367. − [8g] R. W. Redmond, C. W. Harwig, J. C. Scaiano, *Photochem. Photobiol. A* **1992**, *68*, 255−259. − [8h] J. C. Netto-Ferreira, V. Wintgens, J. C. Scaiano, *Tetrahedron Lett*. **1989**, *30*, 6851−6854. − [8i] J. C. Scaiano, V. Wintgens, J. C. Netto-Ferreira, *Pure Appl. Chem.* **1990**, *62*, 1557−1564. − [8j] D. W. Jones, G. Kneen, *J. Chem. Soc., Perkin Trans. 1* **1975**, 171−174. − [8k] J. M. Holland, D. W. Jones, *J. Chem. Soc. (C)* **1971**, 608−612.

[9] *CKS, Chemical Kinetics Simulator, v. 1.02*, IBM Almaden Research Center, Almaden, **1995**.

[10] W. R. Roth, T. Ebbrecht, A. Beitat, *Chem. Ber.* **1988**, *121*, 1357−1358.

[11] H. Kropf, S. Munke, in *Methoden der Organischen Chemie (Houben-Weyl), vol. E13/2*, 4th Ed., Thieme, Stuttgart, **1988**, p. 1388.

[12] [12a] J. Rigaudy, G. Chelu, N. K. Cuong, *J. Org. Chem.* **1985**, *50*, 4474−4478. − [12b] F. Gobert, S. Combrisson, *Tetrahedron* **1974**, *30*, 2919−2924. − [12c] M. Oyama, K. Nozaki, S. Okazagi, *J. Electroanal. Chem*. **1991**, *304*, 61−73.

[13] J. Wisniak, M. Herskowitz, *Solubility of Gases and Solids, Part B, Physical Sciences Data 18,* Elsevier, Amsterdam, **1984**.

[14] F. Wilkinson, *Pure Appl. Chem*. **1997**, *69*, 851−856.

[15] [15a] G. Porter, M. F. Tchir, *J. Chem. Soc. (A)* **1970**, 1372−1373. − [15b] G. Porter, M. F. Tchir, *J. Chem. Soc., Chem. Commun.* **1971**, 3772−3777. − [15c] G. Quinkert, H.-P. Lorenz, W. W. Wiersdorff, *Chem. Ber.* **1969**, *102*, 1597−1605.

[16] C. Rüchardt, M. Gerst, J. Ebenhoch, *Angew. Chem.* **1997**, *109*, 1474−1498; *Angew. Chem. Int. Ed. Engl.* **1997**, *36*, 1406−1430.

[17] H. H. Perkampus, *UV-Vis Atlas of Organic Compounds, Part 2*, 2nd ed., VCH, Weinheim, **1992**, p. 622.

[18] [18a] R. Boese, D. Bläser, *Angew. Chem*. **1988**, *100*, 293−295; *Angew. Chem. Int. Ed. Engl*. **1988**, *27*, 304−306. − [18b] F. Toda, K. Tanaka, Z. Stein, I. Goldberg, *Acta Crystallogr. Sec. C* **1996**, *52*, 177−180.

[19] J. J. P. Stewart, *J. Comput. Chem*. **1989**, *10*, 109−220.

[20] [20a] E. F. Ullman, K. R. Huffman, *Tetrahedron Lett.* **1965**, *23*, 1863−1867. − [20b] R. M. Wilson, K. Hannemann, K. Peters, E.-M. Peters, *J. Am. Chem. Soc*. **1987**, *109,* 4741−4743.

[21] *WINSIM*, Author: D. R. Duling, Laboratory of Molecular Biophysics, NIEHS, NIH, Research Triangle Park, North Carolina; see: D. R. Duling, *J. Magn. Reson. B.* **1994**, *104*, 105−110.

[22] H. Kurrek, B. Kirste, W. Lubitz, *Electron Nuclear Double Resonance Spectroscopy of Radicals in Solution*, VCH, Weinheim, **1988**.

Received September 18 1998
[O98423]